https://doi.org/10.1051/epjap/2018180115

EPJ manuscript No.
(will be inserted by the editor)

Effect of noise on measurements of diffusivity in transparent liquid mixtures by digital speckle photography

Cinzia De Leo [a], Domenica Paoletti, and Dario Ambrosini

DIIIE, University of L'Aquila, P.le Pontieri 1, I-67040 L'Aquila, Italy

Received: date / Revised version: date

Abstract. Interfacing two liquid mixtures in a diffusion cell induces noise in the initial state of the diffusing system, that produces a gap between the initial diffusing boundary and the ideally boundary assumed in the theory. Measured diffusivity values systematically drift with time and they are often corrected by using a linear shift of the zero-time of the process at sufficiently long times, when the system reaches the free one-dimensional diffusive regime. In data analysis methods which involve correlation between pairs of successive digital images of the cell, it is not easy to establish how long the transient lasts. We show that when the initial perturbation between solution and solvent relaxes slowly toward the diffusive regime, no simple zero-time correction can be applied.

PACS. PACS-key discribing text of that key – PACS-key discribing text of that key

1 Introduction

Diffusion is a molecular mass transport process which in transparent media can be suitable studied by optical imaging techniques, that have a long tradition in visualization and in flow analysis, being sensitive and non destructive investigation techniques. A standard method for measuring the diffusion coefficient in liquid binary mixtures is that of observing a free unidimensional diffusion process: a sharp concentration gradient is first set up between two liquids, solution and solvent. Then, the decay of this gradient is observed illuminating the cell with a laser light beam in a direction perpendicular to the gradient. The dynamics of the decaying process is described by Fick's second law of diffusion, with the initial condition that referred to the Heaviside step function for the concentration distribution. A measurement of the time evolution of the refractive index or of the refractive index gradient profile gives an estimate of the mass diffusion coefficient [1].

Different experimental methods have been developed to form an initial sharp diffusion boundary, such as by using a diaphragm cell [2], the critical temperature to make fluids in two initial immiscible phases [3] or fluid injection procedures controlled by capillary tubes [4].The common objective is to set up the initial state reducing at minimum any source of noise, which tend to perturb the relaxation process of the concentration gradient. In any case, the initial experimental state differs from the theoretical one, being a hard task to place two miscible liquids in a Heaviside step initial state. The gap, between experimental observations and theoretical predictions, systematically induces a noise on the measured value of the diffusion coefficient.

In order to bypass this problem, Longsworth [5] has proposed modelling the initial experimental state as an initial mixing state, and to extrapolate the zero time of the theoretical initial step by a linear fit on data distribution as a function of time, for sufficient enough time from the initial time. The zero-time linear shift correction is then the time interval that must be added to the recorded time in order to obtain the correct value of the diffusion coefficient. The underlying hypothesis of having the whole data set in the unperturbed free diffusive regime is guaranteed by the linear fit on data.

In correlation analysis techniques is not simple to determine if a data sample is all in the unperturbed free diffusive regime in order to applied the zero-time correction. A linear shift of the initial time is sometimes assumed a priori in data analysis methods which involve time correlations between pairs of digital images of the cell, as in optical methods developed to measure the refractive index variation with concentration [3],[6–9]. Moreover, it takes a finite time δt_0 to place two fluids into contact to form the initial state, which also induces uncertainty on fixing the experimental zero time on a reference frame, therefore, δt_0 should be held as low as possible. By using fluid injection procedures, a low value of δt_0 might induce larger noisy fluctuations on the interfacial region of the two liquid mixtures and longer transient dynamics. Longsworth [5] has also warned that, when the boundary between solution and solvent is perturbed over the period of time during which it is being set up, no simple linear zero-time correction might be applied. In this paper we report the result of a data analysis investigation developed to observe the

[a] e-mail:cinzia.deleo@univaq.it

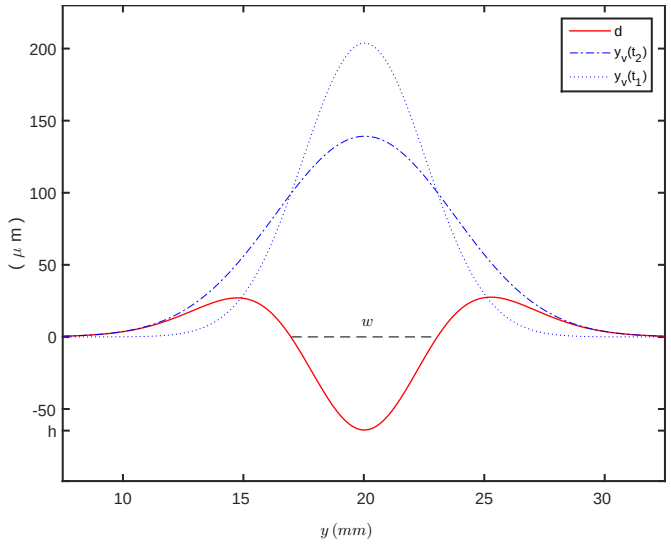

Fig. 1. Absolute and relative profiles of the light ray displacement y_ν observed from the image point y of the cell at the times $t_1 = 35\,min$ and $t_2 = 75\,min$ in a diffusion cell with thickness $\ell = 1.0\,cm$ and diffusion coefficient $D = 1.54 \cdot 10^{-5} cm^2/s$. The relative profile is $d = y_\nu(t_2) - y_\nu(t_1)$.

relaxation process of the concentration gradient in time correlation data analysis in a cell filled by injection. We consider the diffusion of 1.75 M NaCl aqueous solution in pure water while it is undergoing free diffusion in a cell filled through injection. By using Digital Speckle Photography technique [10] we observe the dynamics of speckled patterns generated by a laser light beam which is bent passing through the cell. Speckle's displacements are then measured in the correlation mode developed by the Particle Image Velocimetry (PIV) techniques [11]. We find a noise-to-signal ratio which decays faster than expected in the case of noise modelled by a linear shift of the zero-time but with a long relaxation time, much greater than the injection time, $\tau >> \delta t_0$. We get the mass diffusion coefficient corresponding to the unperturbed free diffusion limit.

2 Theoretical background

Emerging from a point of the exit face of a diffusion cell, a light ray travels a path inside the diffusing medium which depends on the optical properties of the material. The propagation of a light ray in a refractive index field is described by the ray equation [12]:

$$\frac{d}{ds}\left(n\frac{d\boldsymbol{r}}{ds}\right) = \nabla n \tag{1}$$

where $\boldsymbol{r}$ is the vector position of a point on the ray path and s a curvilinear abscissa. In a one-dimensional diffusion process, the refractive index is function of only one spatial variable, $n = n(y,t)$, then the two-dimensional trajectory of a light ray propagating along the optical z-axis of an imaging system, in paraxial approximation, is given by solving the system of differential equations:

$$\frac{d}{ds}\left(n\frac{dz}{ds}\right) = 0 \tag{2}$$

$$\frac{d}{ds}\left(n\frac{dy}{ds}\right) = \frac{dn}{dy} \tag{3}$$

with $ds = \sqrt{(dz)^2 + (dy)^2}$ the arc-length element of the ray path. The resulting equation is:

$$\frac{d^2y}{dz^2} = \frac{1}{2\gamma^2}\frac{dn^2}{dy} \tag{4}$$

where $\gamma = n\,dz/ds = n\,cos\phi$ is constant over the path of the ray, ϕ is the angle that the light ray makes with the optical z-axis. A binary system of two liquid mixtures, solution and solvent, initially separated at the surface $y = y_0$, in a column with rectangular cross section, evolves following Fick's second law. The refractive index field of dilute electrolyte solutions depends linearly on the concentration, and for the given initial and boundary conditions it is expressed by [13]:

$$n(y,t) = n_m - \frac{\Delta n_o}{2}\, erf\left(\frac{y - y_0}{2\sqrt{Dt}}\right) \tag{5}$$

where D is the diffusion coefficient, n_m the refractive index of the fluid at the end of the diffusion process and Δn_o the initial difference between the refractive index of the two liquid mixtures. The initial $t = 0$ state corresponds to a sharp gradient expressed by the Heaviside step function with the solution in the region at $y - y_o \leq 0$.
When $\Delta n_o/2n_m << 1$, one gets from Eq. (4):

$$\frac{d^2y}{dz^2} \simeq \frac{n_m}{\gamma^2}\frac{dn}{dy} \tag{6}$$

while the refractive index gradient, from Eq. (5), has a Gaussian distribution

$$\frac{dn}{dy} = -\frac{\Delta n_o}{\sqrt{4\pi Dt}}\, exp\left[-\frac{(y - y_0)^2}{4Dt}\right] \tag{7}$$

and, therefore, Eq. (6) does not have an analytical solution. For a smooth relaxation of the concentration gradient, the refractive index and its gradient are fairly constant along the path of the ray. At the end of the diffusion cell the bending angle ϕ_ℓ, for a light ray entering the medium in a direction perpendicular to the gradient, is given by

$$tan\,\phi_\ell = \frac{dy}{dz}\Big|_{z=\ell} \simeq \frac{1}{n}\frac{dn}{dy}\,\ell. \tag{8}$$

The ray is focused by a lens on the imaging recorded system of a digital CCD cameras when $tan\,\phi_\ell \sim \phi_\ell$, and a linear backward extension to the input plane gives the virtual position $y_v(t) = y - \ell\,\phi_\ell(t)$ where it is viewed coming in by the CCD matrix at the image point y . A relative displacement d proportional to the change of the

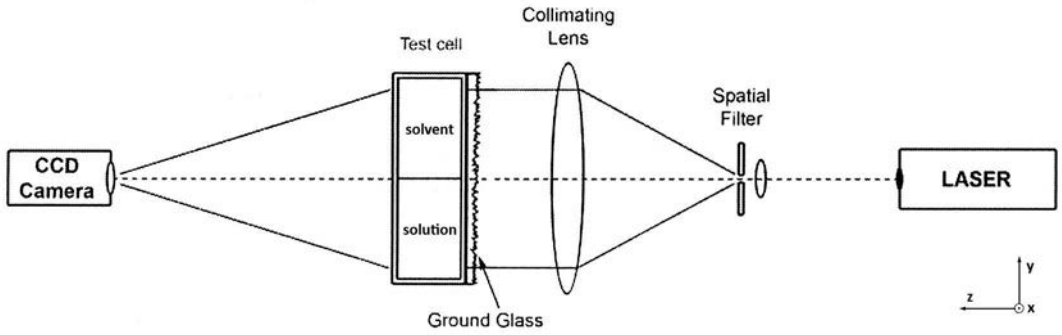

Fig. 2. Experimental set-up for diffusivity measurements by Digital Speckle Photography

ray deflection is observed, at two instances in time t_1 and t_2 [14, 15]:

$$d = y_v(t_2) - y_v(t_1) = \left(\frac{dn}{dy}\Big|_{t_2} - \frac{dn}{dy}\Big|_{t_1} \right) \frac{\ell^2}{n_m}. \quad (9)$$

Figure 1 reports the profile distributions as function of the image position y, which are obtained solving numerically Eq. (6) using a fourth-order-Runge-Kutta method [16] in order to check the assumption made in Eq. (8) for the experimental conditions $\Delta n_o/n_m = 1.3 \times 10^{-2}$. The ray tracing along the cell and the backward extension, from the image position y, are obtained for light beam crossing the cell at times $t_1 = 35$ min and $t_2 = 75$ min for a diffusion process with constant $D = 1.54 \cdot 10^{-5} cm^2/s$ in a cell of thickness $\ell = 1.0\, cm$.

The displacement profile in Eq. (9) has two principal characteristics: the relative distance w between the two turning points of reference $d = 0$, which are related to the maximum and the minimum value of the concentration difference at times t_1 and t_2,

$$w = \sqrt{\frac{8D\, ln(t_2/t_1)}{1/t_1 - 1/t_2}}, \quad (10)$$

and the principal change of the refractive index gradient at $y = y_0$,

$$h = \frac{\Delta n_o}{2n_m} \frac{\ell^2}{\sqrt{\pi D}} \left(\frac{1}{\sqrt{t_2}} - \frac{1}{\sqrt{t_1}} \right). \quad (11)$$

3 Experimental set-up

Figure 2 shows a schematic drawing of the set-up. We use a classical spectrophotometric glass cell of internal dimensions $10\, mm \times 45\, mm$ and path length $\ell = 10\, mm$ along the optical axis. The light source is a laser diode beam of wavelength $\lambda = 638.5\, nm$ and maximal power of 5 mW (Lasiris by Stocker Yale). The laser beam is expanded and then collimated to illuminate the cell. A ground glass diffuser is placed at the laser entrance surface of the cell. When the ground glass diffuser is illuminated by the laser beam the refracted light assumes a speckled pattern characterized by random distribution of scattered light. The phase distribution of this pattern is sensitive to the refractive index changes of the medium through which the light travels [17–19]. Speckled fields are then used in digital image correlation methods to measure the displacements of the laser beam in the refractive index fields of the diffusion cell, they are recorded through a lens on the matrix of the CCD camera Silicon Video 9T001C of 2048×1536 resolution and $3.2\mu m \times 3.2\mu m$ pixel area size. A TEC-55 55mm F/2.8 Telecentric Computar Lens reduces viewing angle error and magnification error providing good resolution and contrast. The speckled pattern visibility and the spatial resolution are optimized for an average speckle diameter of 4 pixels, relative to the pixel size in the camera, and an aperture of $f/8$ of the lens [20].

Experimental measurements are performed considering the diffusion of a 1.75 M (moles l^{-1}) solution of NaCl in pure water at $T = 26^oC$. The ambient air temperature in the room is controlled by the air condition system of the laboratory, the air bath temperature is confirmed near the cell.

In dilute aqueous electrolyte solutions the refractive index increases linearly with the concentration. The specific refractive index increment is $\nu = 1.70 \cdot 10^{-1} ml/g$ for the wavelength $\lambda = 638.5\, nm$, as extrapolated from data in the literature [21]. The refractive ratio for the binary mixtures is then : $\Delta n_o/n_m = \nu \Delta c/(n_o + \nu\, c_m) = 1.301 \cdot 10^{-2}$ where Δc is the initial concentration difference between the solution of NaCl and water, c_m their average value and $n_o = 1.331$ the refractive index of water [22].

The diffusion cell is first half filled with the solvent, pure water, and then the NaCl aqueous solution is slowly injected from the bottom using a capillary tube. Both solution and solvent are allowed to equilibrate at the room temperature before they are injected into the cell. At the end of the injection process, which takes a time interval $\delta t_o \sim 40s$, a sequence of single exposure image are acquired by the CCD camera for eighty minutes of working camera.

Then, pairs of successive image frames are processed off-line by means of image processing analysis based on the cross-correlation technique used in PIV [23] in order to measure the displacement of the refractive index gradient profile that takes place during the time interval that separates the two recorded speckled fields. Local displacements are statistically evaluated by correlating speckles

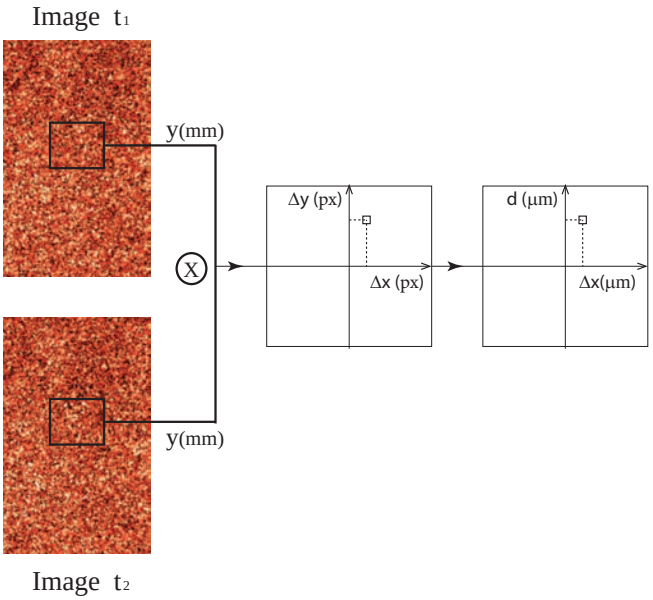

Fig. 3. Schematic representation of the imaging set-up in PIV. The position of the cross-correlation peak gives the displacement.

contained within sub-images, the interrogation windows, placed at the same location of the two successive recorded images. Data analysis are performed using the adaptive cross-correlation algorithm developed by Astarita and his group [24–27], which is based on recursive correlation processing techniques to iteratively arrive at the local displacement, decreasing the interrogation window size during a multipass approach. The final interrogation window size is set to $L_y \times L_x = 10\,pixel \times 50\,pixel$ to obtain a better resolution in the direction of the diffusion, and to have about 30 speckles as statistical sample to reduce the uncertainty of the measurement. The cross-correlation procedure results in a signal peak in the correlation plane, which is a 2-dimensional pixel vector shift. The signal component along the cell diffusion direction y is then set equivalent to the relative ray displacement d of Eq.(9) by the optical magnification of the camera, a schematic graph is given in Fig.2. The camera calibration gives one pixel corresponding to a distance of $12.57\mu m$ along the diffusing cell. Ten pairs of final windows are used for the ensemble averaging, along the horizontal direction x, to get the resulting displacement value.

4 Principles of measurements

An ideal classic one-dimensional free diffusion process starts with two miscible liquids, solution and solvent, initially separated by a sharp horizontal surface $y = y_0$ at the initial time $t = 0$ in a diffusion cell. The variance of the refractive index gradient profile, in Eq.(7), spreads from the initial boundary proportionally to the elapsed time, as $\sigma_t^2 = 2Dt$.

Real diffusion experiments set up the interface between the two liquids mixtures by a procedure, which takes a finite time and blurred the initial diffusing boundary from the ideal boundary assumed in the theory, that produces an uncertainty on fixing the time of the undisturbed diffusing process. The measured diffusivity values D_t drift with time.

The simplest case is when the diffusivity drift can be modelled assuming a linear zero-time shift t_0 from the time $t = 0$ the boundary is experimentally formed and the plot of the measured values D_t against $1/t$ is linear. This effect has been shown for the first time by Longsworth [5] with a Gouy interferometer, by using two dilute electrolyte solutions set up in a Lamm diaphragm cell.

The zero time correction is obtained first by measuring the position of the most deflected ray light as function of time, which is proportional to the maximum height $H_m = \Delta n_0/\sqrt{4\pi D(t-t_0)}$ of the refractive index gradient profile, and then extrapolating linearly to $1/H_m^2 = 0$, which gives the exact zero time t_0 of the process. The zero time is usually located at an earlier time from the time $t = 0$ the boundary is set up, being related to the thickness $\lambda \sim \sqrt{Dt_0}$ of the blurred initial boundary in the diffusion cell. Thus, a constant increment t_0 must be added to the observed time t to obtain the corrected value D of the diffusion coefficient. The drift with time induced on the measured diffusion coefficient, for sufficiently large values of t and in the absence of time correction, is then

$$\frac{\Delta D_d}{D} \sim \frac{t_0}{t} \tag{12}$$

with $\Delta D_d = D_d - D$ where D_d is the diffusion coefficient measured at time t .

In data analysis methods which involve temporal correlation between time points, $t_1 = t$ and $t_2 = t + \Delta t$, the drift with time induced on the measured diffusivity depends on the methods chosen for the estimation of the diffusivity. For example, if the principal relative change h of the refractive index gradient in Eq.(11) is detected then this is:

$$h(t, t+\Delta t, D_h) = h(t+t_0, t+t_0+\Delta t, D)$$

from which follows

$$\frac{\Delta D_h}{D} \sim \left(\frac{1/\sqrt{t} - 1/\sqrt{t+\Delta t}}{1/\sqrt{t+t_0} - 1/\sqrt{t+t_0+\Delta t}} \right)^2 - 1 \tag{13}$$

with $\Delta D_h = D_h - D$, where D_h is now an averaged coefficient in the time interval from t to $t + \Delta t$, at $y = y_0$. Instead, considering the relative distance w between the two turning points expressed by Eq.(10),this is:

$$w(t, t+\Delta t, D_w) = w(t+t_0, t+t_0+\Delta t, D)$$

from which follows

$$\frac{\Delta D_w}{D} \sim \frac{(t+t_0)(t+t_0+\Delta t)}{t(t+\Delta t)} \frac{ln[1+\Delta t/(t+t_0)]}{ln(1+\Delta t/t)} - 1. \tag{14}$$

with $\Delta D_w = D_w - D$, where D_w is now an averaged coefficient in the time interval from t to $t + \Delta t$ and in the

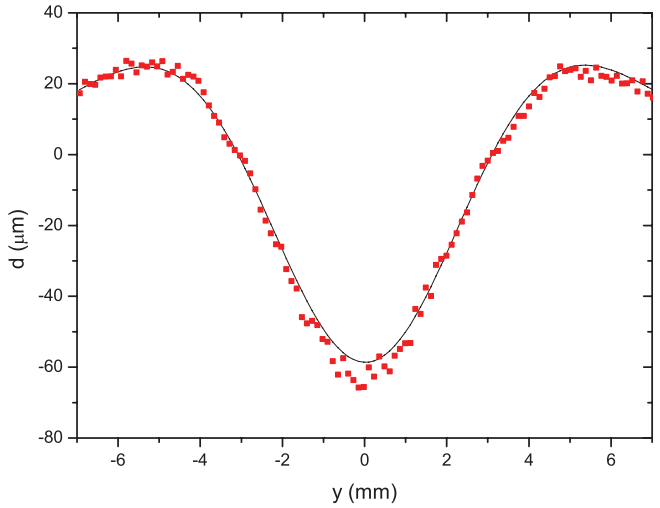

Fig. 4. Experimental data (squares) obtained for diffusion of NaCl solution in pure water with $t_1 = 35min$ and $t_2 = 75\,min$. Solid line is the least square best fit, using Eq.(16);

range $y = y_0 \pm w/2$. In both cases the underlying assumption that the diffusion proceeds undisturbed is not easy to confirm from observed data distributions because now the zero-time of the diffusion process can not be linearly extrapolated from data.

In measurements which involve Gaussian refractive index gradient profiles, a noise can be modelled by adding a noise variance term σ_n^2. Thus, at the time t, the variance of the dynamic process is $\sigma_t^2 = 2Dt + \sigma_n^2 = 2D_t t$. The measured diffusivity D_t is scattered by time as:

$$D_t = D + \sigma_n^2/2t. \tag{15}$$

If the diffusion process evolves undisturbed then the noise variance σ_n^2 is expected to be constant. This is equivalent to having a linear zero time shift $t_0 = \sigma_n^2/2D$ on the measured time t. In order to separate signal from noise, we have extracted the temporal behaviour of the diffusivity D_t, in time correlation analysis, by fitting the experimental displacement profile of the refractive index gradient to the theoretical prediction of Eq. (9) at the two different time correlation points t_1 and t_2. The data profile has been fitted through the least-square method [28] by minimizing the sum of the squares of the differences between data and the model, with the diffusivity D_1 at $t = t_1$ and D_2 at $t = t_2$ as free parameters:

$$d = \frac{\Delta n_o \ell^2}{2n_m\sqrt{\pi}}\Big[\frac{1}{\sqrt{D_2 t_2}} exp\left(-\frac{y^2}{4D_2 t_2}\right) + \\ + \frac{1}{\sqrt{D_1 t_1}} exp\left(-\frac{y^2}{4D_1 t_1}\right)\Big]. \tag{16}$$

The central position, fixed at $y_0 = 0$, had been previously found by using a polynomial fit in order to detect the position of the principal change of the data profile. The spatial interval used for fitting is $[-7mm, 7mm]$ in order to cut off the tail of the gradient profile, at the lower and the upper range, avoiding board effects. Moreover, this interval always encompasses the relative distance w between the two turning points $d = 0$ of Eq. (16), which is now expressed as

$$w = \sqrt{\frac{8\ln(D_2 t_2/D_1 t_1)}{(D_1 t_1)^{-1} - (D_2 t_2)^{-1}}}. \tag{17}$$

Figure 4 shows a comparison between experimental data and the model after fitting. Table 1 reports the values of the apparent diffusion coefficient D_t obtained for different time correlation points t_1 and t_2. The fitting procedure also returns the values of diffusivity for the two regions which are separated by the interface at $y_0 = 0$, these are D_t^+ for positive values of y, and D_t^- for negative values of y, for each of the two values of time t_1 and t_2. The two regions are not symmetric as is expected in the case of an undisturbed free diffusion process. In each region, a small change $\epsilon_t^\pm = D_t^\pm - D_t$ of the diffusivity, at each time, is related to the relative change $\delta^\pm$ of the position of the two turning points of Eq. (16) as

$$\delta^\pm = \sum_{t=1,2} \frac{1}{2}\frac{\partial w}{\partial D_t}\epsilon_t^\pm = \\ = \frac{2}{w[(D_1 t_1)^{-1} - (D_2 t_2)^{-1}]}\Big[\frac{D_1^\pm - D_1}{D_1}(\gamma D_2 t_2 - 1) + \\ + \frac{D_2 - D_2^\pm}{D_2}(\gamma D_1 t_1 - 1)\Big] \tag{18}$$

where $\gamma = (D_2 t_2 - D_1 t_1)^{-1} ln(D_2 t_2/D_1 t_1)$.

In the low concentration region, $y > 0$, we observe $D_1^+ > D_1$ and $D_2^+ < D_2$, which both give $\delta^+ > 0$. Instead, the opposite behaviour is detected in the high concentration region, $y < 0$, where $D_1^- < D_1$ and $D_2^- > D_2$ with $\delta^- \simeq -\delta^+$, which leave the width w almost unchanged. Table 1 depicts evaluated $\delta^\pm$ values at time correlation points t_1 and t_2.

The asymmetry of the diffusivity detected in the two regions decreases with time. This suggests that for sufficiently long times the refractive index gradient profile will converge to the Gaussian profile of the unperturbed free diffusion process. The validity of the zero-time correction depends upon the assumption that the concentration distribution is expressed by Eq. (5) and, then, the gradient distribution is Gaussian.

Figure 5 shows the diffusivity values D_t as function of time, the uncertainty is set equal to the average diffusivity changes ϵ detected in the two regions separated by the boundary $y_0 = 0$. This plot shows that the diffusivity rate of decay is faster than that expected assuming a constant noise variance σ_n^2 in Eq. (15). Therefore, it might be connected to a more complex noise dynamics induced during the injection of fluid in the cell, assuming the diffusion constant independent of concentration.

Fluid injected in a cell can generate long range components of noise, varying temporally and spatially, as a consequence of initial macroscopic caotic environmental fluctuations around the interfacial region and their subsequent decay bounded by gravity and the finite dimensions

Table 1. Diffusivity values at times t_1 and t_2 and relative displacements $\delta^{\pm}$ of the two turning points by Eq.(18). D^+ and D^- are the diffusion coefficients obtained by fitting through Eq.(16) only negative and positive y values, respectively.

t_1 (min)	D_1	D_1^+	D_1^-	t_2 (min)	D_2	D_2^+	D_2^-	δ^+	δ^-
	($10^{-9}m/s^2$)				($10^{-9}m/s^2$)			(%)	
25	1.759	1.794	1.724	50	1.559	1.540	1.580	0.27	-0.24
25	1.716	1.766	1.665	55	1.541	1.524	1.560	0.57	-0.55
30	1.645	1.670	1.621	60	1.570	1.550	1.590	0.14	-0.12
30	1.650	1.670	1.630	65	1.553	1.539	1.567	0.14	-0.14
30	1.665	1.700	1.630	70	1.540	1.530	1.550	0.45	-0.45
35	1.591	1.619	1.561	60	1.524	1.517	1.531	0.37	-0.40
35	1.612	1.640	1.583	65	1.535	1.525	1.545	0.33	-0.34
35	1.635	1.670	1.600	70	1.550	1.540	1.560	0.74	-0.74
35	1.633	1.662	1.602	75	1.540	1.530	1.550	0.35	-0.39
40	1.585	1.611	1.559	80	1.542	1.534	1.550	0.34	-0.34
45	1.553	1.572	1.533	80	1.543	1.535	1.553	0.22	-0.21

of the cross section of the cell. These perturbations are expected to die away through a homogenization process, relaxing toward the dominant dynamic process in the cell. The variance of noise in Eq. (7) is then expected to be time correlated and its decay rate characterizes the fluctuating field [29–31]. As a rough estimation, we fit the data on the plots of Fig. 5 by assuming an exponentially decaying mode of the Gaussian noise variance, $\sigma_n^2 = \lambda^2 exp(-t/\tau)$, with λ related to the initial contour domain of the noise field and τ the mean life time of the decaying process. We model the noise dynamics on the time scale of the diffusion as a superposition of normal mode with different wavelengths with $\lambda = \sqrt{2D\tau}$ the dominant average wavelength, this gives:

$$D_t = D\left[1 + \frac{\tau\ exp(-t/\tau)}{t}\right] \tag{19}$$

where the diffusion coefficient D and the noise life time τ are the fitting parameters. The weighted least square fitting technique is now performed to obtain the corresponding parameter values, with the weights given by the uncertainty on D_t taking into account the different impact of noise on measurements.

The estimated diffusion coefficient, at a confidence level of 95%, is $D = (1.539 \pm 0.013) \cdot 10^{-9}m^2/s$. The mean life time of decaying noise field is $\tau = (15 \pm 2)min$, which is much greater than the injection time $\delta t_0 = 0.67min$, it could be considered as the timescale crossover to the unperturbed free diffusion process. The dimension of our sample, data collected up to time $t = 80\,min$, is not large enough to be also sensitive to the zero-time correction in the unperturbed free regime.

5 Conclusion

There are few data available to check the result. The most useful are those obtained by Riquelme et al. [32], through optic interferometric measurements, in similar experimental condition of the binary mixture and the diffusion cell. They have developed two methods to measure the diffusion coefficient in time correlation data analysis. They have also detected asymmetry of the diffusion coefficients at positive and negative y values. No zero-time correction was applied to their data.

Results were $D = (1.587 \pm 0.05) \cdot 10^{-9}m^2/s$ and $D = (1.602 \pm 0.05) \cdot 10^{-9}m^2/s$, both are in agreement with the behaviour of the mean value and the standard deviation of all our diffusivity values reported in the Table 1: $< D_t >= (1.593 \pm 0.064) \cdot 10^{-9}m^2/s$.

Riquelme et al.[32] also extrapolated some experimental data from literature to obtain expected values of the diffusion coefficient in order to compare them with their experimental results. The extrapolated values are in the range $(1.522 - 1.559) \cdot 10^{-9}m^2/s$.

In this range we also find the diffusion coefficient value $D = (1.539 \pm 0.013) \cdot 10^{-9}m^2/s$ obtained by extrapolating the diffusivity data sample in Fig. 5 toward the unperturbed one-dimensional diffusion regime. No zero-time correction was applied.

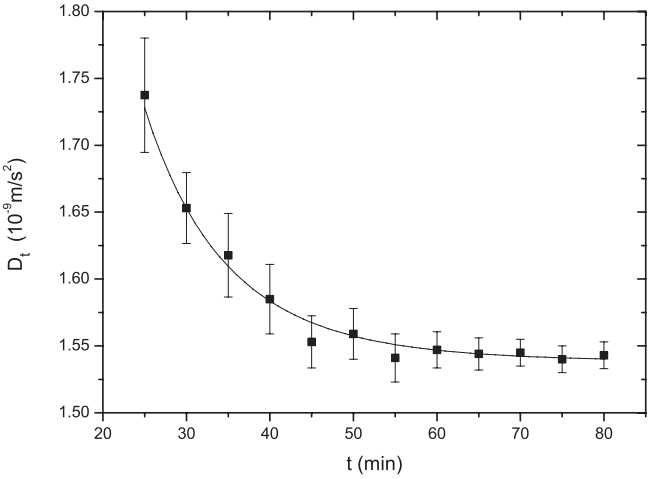

Fig. 5. The diffusivity D_t as function of time. Solid line is the weighted least square best fit, using Eq.(19);

6 Authors contributions

All the authors were involved in the preparation of the manuscript. All the authors have read and approved the final manuscript.

References

1. D. Ambrosini, D. Paoletti, and N. Rashidnia, Opt. Las. Engin. **4**6, 852 (2008)
2. R.H. Stokes, J. Am. Chem. Soc. **7**2, 763 (1950)
3. N. Bochner and J. Pipman, J. Phys D Appl. Phys. **9**(13), 1825 (1976)
4. L. Gabelmann-Gray and H. Fenichel, Appl. Opt. **1**8(3), 343 (1976)
5. L. Longsworth, J. Am. Chem. Soc. **6**9, 2510 (1947)
6. A.Mialdun and V. Shevtsova, J. Chem. Phys. **1**34(4), 044524 (2011)
7. A.Mialdun, V. Sechenyh, J.C. Legros, J.M. Ortz de Zárate, and V. Shevtsova, J. Chem. Phys. **1**34(10), 104903 (2013)
8. M.G. He,S. Zhang, Y. Zhang, and S.G. Peng, Opt. Express **2**3(9), 10884 (2015)
9. S. Zhang,M. He, Y. Zhang, S. Peng,and X. He, Appl. Opt. **5**4, 9127 (2015)
10. N.A. Fomin, *Specle Photography for Fluid Mechanics Measurements* (Springer-Verlag, 1998)
11. J. Westerweel and R.J. Adrian, *Particle Image Velocimetry* (Cambridge University Press, 2011)
12. V. Lakshminarayanan, A. Ghatak and K. Thyagarajan, *Lagrangian Optics* (Springer Science, 2002)
13. J.Crank, *The mathematics of diffusion* (Oxford University Press, 1975)
14. G. Schirripa Spagnolo, D. Ambrosini, A. Ponticiello, and D. Paoletti, J. Phys. III France **6** 1117 (1996)
15. D. Ambrosini, D. Paoletti, A. Ponticiello and G. Schirripa Spagnolo, Opt. Las. Engin. **3**7, 341 (2002)
16. E.Hairer, C.Lubich, and G.Wanner, *Geometric numerical integration,* (Springer-Verlag, 2006)
17. U. Köpf, Opt. Commun. **5**, 347 (1972)
18. D. Paoletti, G. Schirripa Spagnolo, and D. Ambrosini, J. Phys. III France **2**,1835 (1992)
19. G. Schirripa Spagnolo, D. Ambrosini, and D. Paoletti, Eur. Phys. J. AP **6**,281 (1999)
20. J.W. Goodman, *Speckle Phenomena in Optics: Theory and Applications* (Roberts and Co., 2006)
21. A. Kruis, Z. physik. Chem.**3**4, 13 (1936)
22. L.W. Tilton and J.K. Taylor, J. Res. Natl. Bur. Stand. **2**0, 419 (1938)
23. R.D. Keane, and R.J. Adrian, Appl. Sci. Res. **4**9, 191 (1992)
24. T. Astarita,and G. Cardone, Exp. Fluids **3**8, 233 (2005)
25. T. Astarita, Exp. Fluids **4**0, 977 (2006)
26. T. Astarita, Exp. Fluids **4**5, 257 (2008)
27. F. Avallone, S. Discetti, T. Astarita, and G. Cardone, Exp. Fluids **5**6, 1 (2015)
28. G. Cowan, *Statistical Data Analysis* (Oxford University Press, 1998)
29. J. Ottino, *The kinematics of mixing: stretching, chaos, and transport* (Cambridge University Press, 1989)
30. V. Toussaint, P. Carriere, J. Scott and J.-N. Gence, Phys. Fluids **1**2, 2834 (2000)
31. W. Liu and G. Haller, Physica D **1**88, 1 (2004)
32. R. Riquelme, I. Lira, C. Perez-Lopez, J.A. Rayas and R. Rodriguez-Vera, J. Phys. D Appl. Phys **4**0 (9), 2769 (2007)